This paper is available on line at http://www.mcponline.org

The Metacaspase (Mca1p) has a Dual Role in Farnesol-induced Apoptosis in *Candida albicans*

Thibaut Léger‡, Camille Garcia‡, Marwa Ounissi‡, Gaëlle Lelandais§, and Jean-Michel Camadro‡§¶

Manipulating the apoptotic response of *Candida albicans* may help in the control of this opportunistic pathogen. The metacaspase Mca1p has been described as a key protease for apoptosis in *C. albicans* but little is known about its cleavage specificity and substrates. We therefore initiated a series of studies to describe its function. We used a strain disrupted for the *MCA1* gene (*mca1*Δ/Δ) and compared its proteome to that of a wild-type isogenic strain, in the presence and absence of a known inducer of apoptosis, the quorum-sensing molecule farnesol. Label-free and TMT labeling quantitative proteomic analyses showed that both mca1 disruption and farnesol treatment significantly affected the proteome of the cells. The combination of both conditions led to an unexpected biological response: the strong overexpression of proteins implicated in the general stress. We studied sites cleaved by Mca1p using native peptidomic techniques, and a bottom-up approach involving GluC endoprotease: there appeared to be a "K/R" substrate specificity in P1 and a "D/E" specificity in P2. We also found 77 potential substrates of Mca1p, 13 of which validated using the most stringent filters, implicated in protein folding, protein aggregate resolubilization, glycolysis, and a number of mitochondrial functions. An immunoblot assay confirmed the cleavage of Ssb1p, a member of the HSP70 family of heat-shock proteins, in conditions where the metacaspase is activated. These various results indicate that Mca1p is involved in a limited and specific proteolysis program triggered by apoptosis. One of the main functions of Mca1p appears to be the degradation of several major heat-shock proteins, thereby contributing to weakening cellular defenses and amplifying the cell death process. Finally, Mca1p appears to contribute significantly to the control of mitochondria biogenesis and degradation. Consequently, Mca1p may be a link between the extrinsic and the intrinsic programmed cell death pathways in *C. albicans*. ***Molecular & Cellular Proteomics 14: 10.1074/mcp.M114.041210, 93–108, 2015.***

Apoptosis, or programmed cell death (PCD)[1] is an important physiological process involved in key steps of the development of multicellular organisms. It also regulates the fate of cell populations in adverse conditions. Several pathways have been described involving internal triggering factors, often associated with critical alterations of mitochondrial structures and functions, or external signals received by specific cell death receptors. Apoptosis involves a number of cellular processes including active mechanisms of chromatin condensation, DNA fragmentation, and phosphatidylserine externalization to the outer leaflet of the plasma membrane. Mitochondria appear to be major actors in the intrinsic apoptosis pathway: the alteration of mitochondrial membrane permeability, a Bax-Bcl2-dependent process in mammalian cells, induces overproduction of reactive oxygen species (ROS) and the release of cytochrome *c*, which in turn contribute to the induction of endoproteolytic cascades leading to cell death (1, 2). Caspases are cysteine-proteases acting as key components of apoptosis machineries. In mammalian cells, proforms of the effector caspases 9 and 3 are cleaved and activated, and in turn activate many other cellular caspases (3–5). In mammals, these proteases cleave preferentially after aspartic acid residues (6, 7). Unicellular eukaryotes, including yeasts, also display apoptosis or PCD (8, 9). The yeast *Candida albicans*, which is characterized by a yeast-hyphae dimorphism, is an opportunistic human pathogen responsible for benign candidiasis to life-threatening systemic infections. PCD was shown to be involved in the regulation of collective cellular interactions during biofilm formation by *C. albicans* where cell density is high, and competition for nutrients may occur (10). Under such

From the ‡Mass spectrometry Laboratory, Institut Jacques Monod, UMR 7592, Univ Paris Diderot, CNRS, Sorbonne Paris Cité, F-75205 Paris, France; §Mitochondria, Metals and Oxidative Stress group, Institut Jacques Monod, UMR 7592, Univ Paris Diderot, CNRS, Sorbonne Paris Cité, F-75205 Paris, France

Received, May 14, 2014 and in revised form, October 14, 2014

Published, MCP Papers in Press, October 27, 2014, DOI 10.1074/mcp.M114.041210

Author contributions: T.L. and J.-M.C. designed research; T.L., C.G., M.O., and J.-M.C. performed research; T.L., C.G., M.O., G.L., and J.-M.C. analyzed data; T.L. and J.-M.C. wrote the paper.

[1] The abbreviations used are: PCD, Programmed cell death; ROS: Reactive oxygen species; HSP, Heat-shock proteins; PI, Propidium iodide; TUNEL, Terminal deoxynucleotidyl transferase dUTP nick end labeling; TMT, Tandem Mass Tag; MS/MS, Tandem Mass Spectrometry; FDR, False Discovery Rate.

adverse conditions, *C. albicans* secretes metabolites including farnesol or tyrosol that act as quorum sensing compounds (11, 12). Farnesol has been shown to inhibit biofilm formation (13) and induce ROS production and apoptosis (10, 14) through the activation of a number of signaling pathways, including the Ras c-AMP pathway (15), and Czf1p and Efg1p coordinated activities (16). However, the effects of farnesol may vary according to the growth conditions and physiology of the cells (16), and this has led to some apparently contradictory reports in the literature. For example, in *C. albicans* yeast cells, proteomic studies based on 2D-gel electrophoresis indicate that farnesol increases the expression of heat shock proteins including Cta1p, Hsp90p, and Hsp70p (10). However, in *C. albicans* biofilm, transcriptomic analysis identified down-regulation of the corresponding genes (11). Hsp90p is also involved in *C. albicans* apoptosis by regulating the calcineurin–caspase apoptotic pathway (17). Recent work shows that the effects of farnesol may be mediated by the ABC multidrug transporter Cdr1p-dependent glutathione efflux from cells (18), promoting the conditions for a severe oxidative stress, a triggering signal for apoptosis.

A key player in apoptosis in *C. albicans* is the cysteine-protease Mca1p, a member of the family of metacaspases, a group of specific caspases present in plants, fungi, and protozoans where they have also been implicated in apoptosis (19–21). In *C. albicans*, the *MCA1* gene is the only gene encoding a metacaspase and its activation during apoptosis events has been demonstrated (10). Farnesol induces expression of the *MCA1* gene and leads to the activation of the metacaspase activity at the protein level (10). *C. albicans* lacking Mca1p displays resistance to oxidative stress-induced death and changed energy metabolism (22). Mca1p share 55% sequence identity and 69% overall homology with the metacaspase Yca1p from *Saccharomyces cerevisiae*. Besides its role in the H_2O_2-induced apoptosis, Yca1p has been implicated in other functions: the regulation of the composition of the insoluble proteome with or without H_2O_2 stress (23); clearance of insoluble protein aggregates (24); and cell cycle progression and particularly in G2/M transition (25). Only one substrate of the *S. cerevisiae* Yca1p has been clearly demonstrated, the glycolytic enzyme glyceraldehyde-3-phosphate dehydrogenase (26). However, little is known about Mca1p in *C. albicans*, and in particular about its specificity or direct targets. This is an important issue, because although compounds such as Plagiochin E (27) induce *C. albicans* apoptosis through a caspase-dependent process, others induce apoptosis through metacaspase-independent pathways (28). Indeed, the precise role of Mca1p in the induction of apoptosis and in mitochondrial functions remains unclear. Therefore, we studied the function of Mca1p to decipher in particular the relative contribution of Mca1p and farnesol in the observed variations of the *C. albicans* proteome. We used a strain deleted for the *MCA1* gene (*mca1*Δ/Δ) and compared its proteome to that of a wild-type strain, in the absence and in the presence of the quorum sensing molecule farnesol. We combined classical bottom-up and label-free proteomic techniques using trypsin to identify differences in protein levels. We also developed top-down and bottom-up approaches based on GluC digestion to identify and quantify potential metacaspase targets. This analytical pipeline allowed us to provide new insights into Mca1p function and its involvement in apoptosis in *C. albicans.*

EXPERIMENTAL PROCEDURES

Strains and Growth Conditions—*C. albicans* strains BWP17 (29) and BWP17-*mca1*Δ/Δ (*mca1*Δ::*FRT*/*mca1*Δ::*FRT*) (28) were grown in yeast-extract peptone dextrose (YPD) medium (1% [w/v] yeast extract, 2% [w/v] peptone, and 2% [w/v] dextrose). Cell cultures (100 ml) were inoculated at an initial OD_{600} of 0.1 with liquid precultures (10 ml medium inoculated with freshly grown colonies on YPD agar plates) and incubated in an orbital shaker at 30 °C. Farnesol (250 μM final concentration), or solvent, was added to the cultures in mid-exponential phase of growth, and the cells collected by centrifugation 4h later. *C. albicans* grew as budding-yeast under these conditions. Stock solutions (250 mM) of farnesol (mixed isomers; Sigma Chemical Co, 5 M solution.) were prepared in methanol just before use. Cell-free extracts were prepared by disrupting the cells (60% wet weight/vol in 0.1 M potassium phosphate buffer, pH 7.2) using a One-Shot apparatus (Constant Systems Ltd, Daventry, UK) operating at 2.5 Kbar. The cell lysate was diluted twice in the same buffer, and large cell debris was removed by centrifugation for 10 min at 5000 × *g*. The supernatant, referred to hereafter as the cell homogenate, was rapidly frozen in 5 mg proteins/ml aliquot fractions and kept at −80 °C.

Validation of the Apoptosis Condition by Flow Cytometry—Cells from the four growth conditions (WT, WT-farnesol, *mca1*Δ/Δ, and *mca1*Δ/Δ-farnesol) were collected by centrifugation and washed twice in 1× PBS. Flow cytometry (BD Accury, 10,000 cell counts, medium flow rate) was used in the following ways to evaluate apoptosis: (1) Aliquots were labeled with propidium iodide (PI) at a concentration of 10 μg/ml incubated in the dark for 1h, washed by centrifugation, and counted. (2) Two aliquots were processed to prepare protoplasts. The cells were first preincubated for 10 min at 30 °C in a 0.1 M Tris-Cl buffer containing 0.5 M 2-mercaptoethanol. The cells were washed in 0.01 M Tris-Cl, pH 7, 0.5 M KCl, collected by centrifugation, and resuspended in the digestion buffer (0.01 M citrate-phosphate buffer, pH 5.8, 1.35 M sorbitol, and 1 mM EGTA). Zymolyase 100T (MP Biomedicals, Illkirch-Graffenstaden, France) was added to a final concentration of 10 mg/ml. The samples were incubated at 30 °C and protoplast formation evaluated by measuring the OD_{600} of 1/100 dilutions of the cells in water. After nearly complete protoplast formation (>85%) the cells were collected by centrifugation and washed in a 0.01 M Tris-maleate buffer, pH 6.8, 0.75 M sorbitol, 0.4 M mannitol, and 2 mM EGTA. An aliquot of the protoplasts was incubated with 5 μl of the annexin V-FITC reagent (BD Pharmingen, San Diego, CA) for 1h in the dark, washed, and then diluted in the same buffer for flow cytometry analysis. Another aliquot was processed for TUNEL labeling: the protoplasts were first fixed with a freshly prepared 4% formaldehyde solution in PBS, permeabilized using 0.1% Triton X-100 in 0.1% (w/v) sodium citrate solution, and further processed with enzyme and reagents from the Roche Cell-Death detection kit according to the manufacturer's instructions (3). Changes in total reduced glutathione concentration were evaluated by a modification of the method of Lewicki *et al.* (30), using naphthalene 2,3 dicarboxaldehyde (NDA) as a glutathione-specific fluorogenic reagent. Intact cells were washed in PBS, incubated with NDA (1 mM) for 30 min in the dark, and analyzed by flow cytometry as described above.

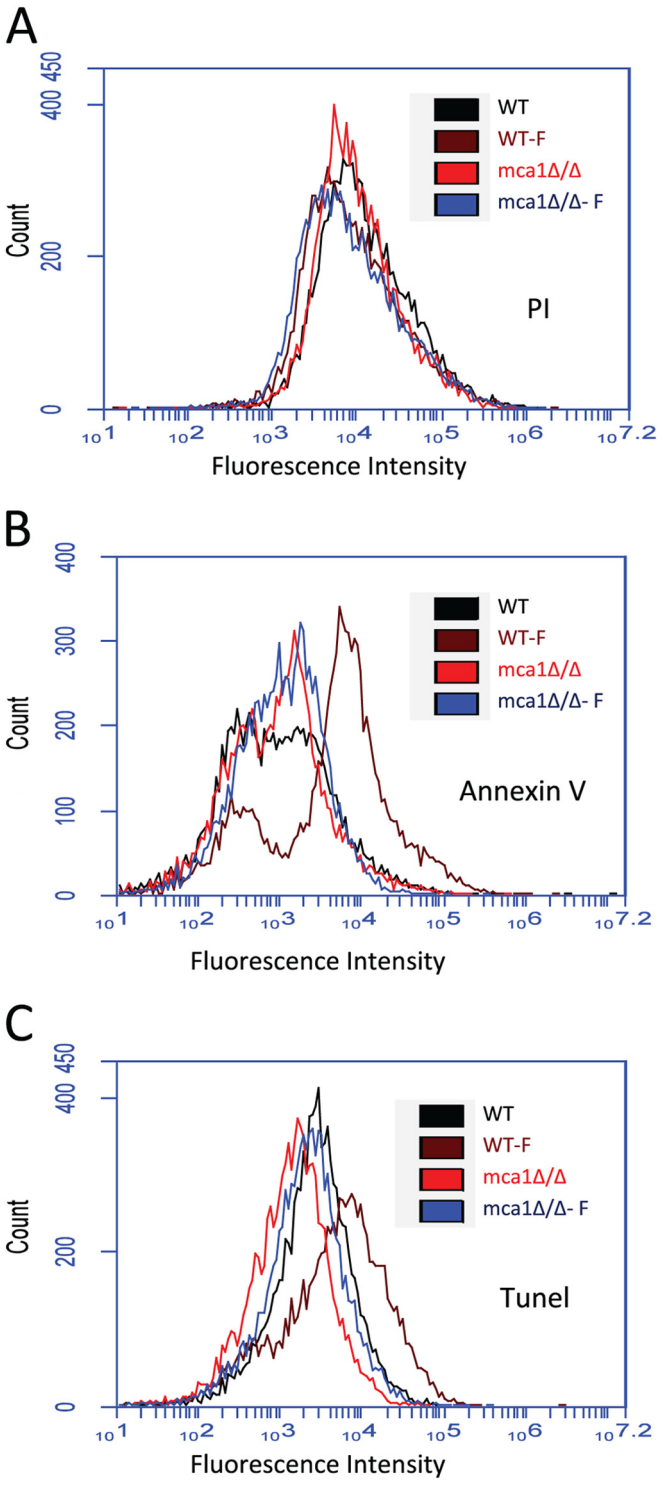

FIG. 1. **Analysis of apoptosis by flow cytometry (specific fluorescence intensity *versus* cell count) in WT and *mca1*Δ/Δ cells grown in the presence or absence of farnesol.** *A*, PI labeling of intact cells, *B*, Annexin V-FITC labeling of fixed protoplasts, and *C*, TUNEL labeling of fixed protoplasts.

SDS-PAGE—Samples of 20 μg of protein prepared from cells in the various conditions investigated were run on a NUPAGE 4–12% acrylamide gel (Invitrogen) and stained in Coomassie blue (Simply-blue Safestain; Invitrogen, Carlsbad, CA).

Western blot Analyses—20 μg protein samples of prepared from cells in the various conditions investigated were separated on a NUPAGE 4–12% acrylamide gel (Invitrogen) and transferred to nitrocellulose membrane (Protran BA85, GE Healthcare Life Sciences). Ssb1p protein expression was assessed by immunoblot with a primary antibody (rabbit polyclonal IgG fraction) raised against the purified protein from *S. cerevisiae* anti-Ssb1p (kind gift from Dr Véronique Albanese, Institut Jacques Monod, Paris). We used an anti-rabbit Horseradish peroxidase conjugated antibody (Sigma Aldrich) and an enhanced chemiluminescent reagent (West Pico, GE Healthcare) for detection.

Strategy for the Analysis of Proteome Variations as a Function of the Experimental Conditions—The general strategy for the production of the different data sets and their exploration is summarized in Fig. 2. The individual steps of this pipeline are described in the following sections.

LC-MS/MS Acquisition—All digests or protein extracts were analyzed using a LTQ Velos Orbitrap equipped with an EASY-Spray nanoelectrospray ion source and coupled to an Easy nano-LC Proxeon 1000 system (all devices are from Thermo Fisher Scientific, San Jose, CA). Chromatographic separation of peptides was performed with the following parameters: Acclaim PepMap100 C18 precolumn (2 cm, 75 μm i.d., 3 μm, 100 Å), Pepmap-RSLC Proxeon C18 column (50 cm, 75 μm i.d., 2 μm, 100 Å), 300 nl/min flow, gradient rising from 95% solvent A (water, 0.1% formic acid) to 35% solvent B (100% acetonitrile, 0.1% formic acid) in 217 min followed by column regeneration for 23 min giving a total run time of 4 h. Peptides were analyzed in the orbitrap in full ion scan mode at a resolution of 30,000 (at *m/z* 400) and with a mass range of *m/z* 400–1800. Fragments were obtained with a collision-induced dissociation (CID) activation with a collisional energy of 40%, an isolation width of 2 Da, and an activation Q of 0.250 for 10 ms. MS/MS data were acquired in the linear ion trap in a data-dependent mode in which the 20 most intense precursor ions were fragmented, with a dynamic exclusion of 20 s, an exclusion list size of 500 and a repeat duration of 30 s. The maximum ion accumulation times were set to 100 ms for MS acquisition and 50 ms for MS/MS acquisition. All MS/MS data were processed with an in-house Mascot search server (Matrix Science, Boston, MA; version 2.4.1). The mass tolerance was set to 7 ppm for precursor ions and 0.5 Da for fragments. The following modifications were used in variable modifications: oxidation (M), phosphorylation (STY), acetylation (K, N-term), and deamidation (N, Q). Glutathionylation (C) was added for additional analyses of trypsin digests. The maximum number of missed cleavages by trypsin was limited to two for all proteases used. MS/MS data were searched against a *C. albicans* ORF database (# 6209) retrieved from the Candida Genome Database website (31) (http://www.candidagenome.org/).

Quantitative Analysis in Label-free Experiments—Proteins in the various homogenates were digested in solution, in duplicate, overnight at 37 °C by sequencing grade trypsin (12.5 μg/ml; Promega, Madison, WI) in 20 μl of 25 mmol/L NH_4HCO_3. LC-MS/MS acquisition was performed with a 4-hour gradient. MS/MS data were processed with an in-house Mascot search server (Matrix Science, Boston, MA; version 2.4.1). Label-free quantification in between subject analysis was performed on raw data with Progenesis-LC software 4.1 (Nonlinear Dynamics Ltd, Newcastle, U.K.) using the following procedure: (1) chromatograms alignment, (2) peptide abundances normalization, (3) statistical analyses of features, and (4) peptides identification using the Mascot server. A decoy search was performed and the significance threshold was fixed to 0.05. The resulting files were imported

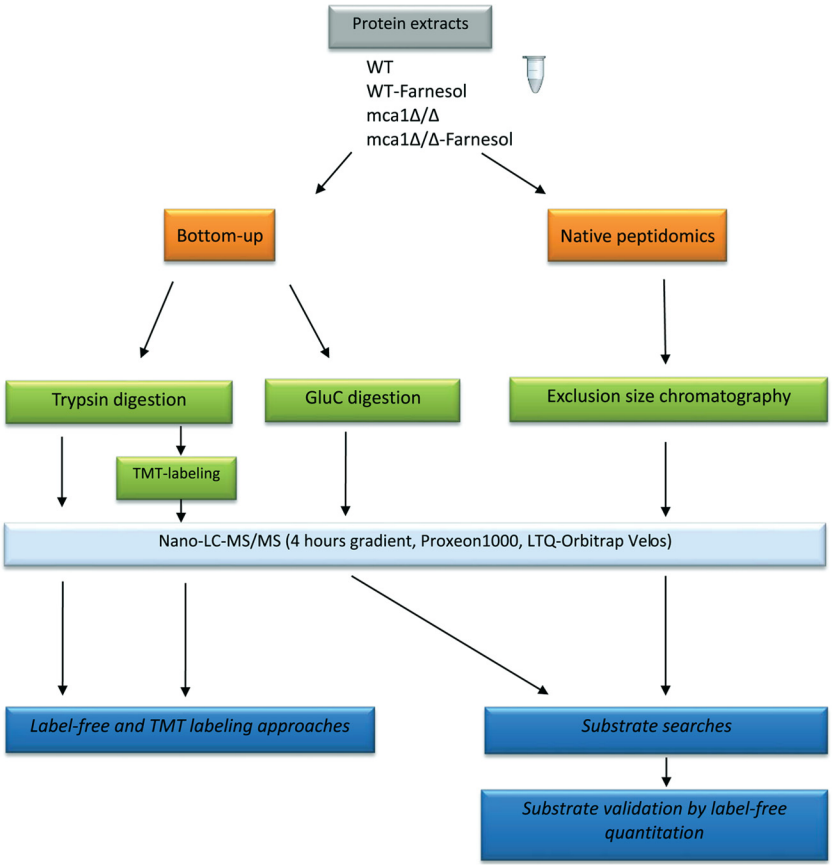

FIG. 2. **Scheme of the study workflow.**

into Progenesis-LC software. Peptides with an ion score less than 15 were rejected. Conflicts for the identification of some peptides were resolved manually. Proteins with similar normalized abundance variations (ANOVA p-value lower than 0.05) were classified by the AutoClass Bayesian clustering system (webserver Autoclass@IJM, http://ytat2.ijm.univ-paris-diderot.fr/)(32). Farnesol and mutation effects were investigated with a two-factor analysis. p-values associated were calculated with a dedicated R script. Gene ontology analyses were performed on all clusters obtained with the GO Slim mapper from the Candida Genome Database website. Functional enrichments for each GO slim term were calculated, relative to the whole identified proteome, using the hypergeometric distribution.

Quantitative Analysis by TMT Labeling Experiments—Aliquots of 100 μg of protein from each cell homogenate preparation were reduced with 10 mM Tris(2-carboxyethyl)phosphine hydrochloride (TCEP), alkylated with 18 mM iodoacetamide according to the TMT sixplex kit protocol (Thermo Fisher scientific, San Jose, CA) then digested in solution overnight at 37 °C by sequencing grade trypsin (12.5 μg/ml; Promega) in 20 μl of 25 mmol/L triethyl ammonium bicarbonate (TEAB). Samples from the WT, WT-farnesol, *mca1*Δ/Δ, and mca1Δ/Δ-farnesol conditions were labeled with 126 (monoisotopic m/z = 126.12773), 127 (m/z = 127.13108 Da), 128 (128.13444 Da), and 129 (m/z = 129.13779 Da) labels, respectively. The samples were mixed, desalted, and concentrated with a 50 mg C18 SPE column (Biotage, Uppsala, Sweden) and the peptides precipitated with acetone. The resulting peptide mixtures were analyzed in triplicate by LC-MS/MS with a 4-hour gradient. MS/MS were acquired with HCD fragmentation and the orbitrap analyzer set at a resolution of 7500 at m/z 400 in a top20 protocol. The maximum ion accumulation time was set to 100 ms for MS acquisition and 50 ms for MS/MS acquisition. Data were processed with Proteome Discoverer 1.4 software (Thermo Fisher scientific, San Jose, CA) and the Mascot search engine with the trypsin digest parameters described above and the additional modifications carbamidomethylation (C) and TMTsixplex (K and N-term). The precursor mass tolerance threshold was set at 0.7 ppm and 0.02 Da for fragment tolerance. The percolator node was used and a 5% FDR was applied. Quantification results in triplicate were treated as replicates and were visualized with Proteome Discoverer 1.4 to allow comparisons with the results obtained by label-free methods.

Peptide Analysis by Native Peptidomic Techniques—Aliquots of 500 μg of protein from cell homogenates from each condition were resuspended (in duplicate) in 1 ml of 50 mM NH_4HCO_3 buffer. Size-exclusion chromatography was performed with a 10 kDa cut-off Amicon membrane (Millipore). Peptides and proteins under 10 kDa were isolated and concentrated with a Speedvac and resuspended in 0.1% formic acid. Peptides were isolated and concentrated with five zip-tip C18 tips for each condition. Peptides were analyzed by LC-MS/MS with a 4-hour gradient. MS/MS data were processed with Proteome Discoverer 1.4 software (Thermo Fisher Scientific) and the Mascot search engine with a "no enzyme" search parameter. The percolator node was used for FDR evaluation with a 5% filter in relaxed FDR and 1% in strict FDR. Peptides were flagged as identified when present in at least one condition with a Q-value under 0.05. The Venny web resource (http://bioinfogp.cnb.csic.es/tools/venny/) was used to produce graphical outputs and visualize specific peptides from different conditions.

Analysis of Peptide Occurrence by a Bottom-up Approach—Triplicate samples from the four conditions were reduced with 10 mM dithiothreitol, alkylated using 55 mM iodoacetamide and digested

TABLE I
Peptides and proteins identified in the four samples (WT, WT-F, mca1Δ/Δ and mca1Δ/Δ-F) in all data sets found with Proteome Discoverer 1.4 and the Mascot search engine 2.4.1 with a 5% FDR threshold

Conditions	WT	WT-Farnesol	*mca1*Δ/Δ	*mca1*Δ/Δ-Farnesol	Total
Trypsin digest (trypsin)	2435 (10407)	2634 (12469)	2558 (12008)	2525 (11790)	3190 (17192)
TMT labeling (trypsin)	–	–	–	–	1601 (7832)
GluC digest (semi-GluC)	882 (5018)	779 (3910)	797 (4274)	838 (3659)	1261 (8549)
Native peptidomics (no enzyme)	85 (220)	66 (146)	64 (143)	52 (113)	137 (416)

overnight at 37 °C by the GluC protease (12.5 μg/ml; Sigma Aldrich) in solution in 20 μl of 20 mM sodium phosphate buffer, pH7.8. The resulting peptides were analyzed by LC-MS/MS with a 4-hour gradient. MS/MS data were processed with Proteome Discoverer 1.4 software (Thermo Fisher scientific, San Jose, CA) and the Mascot search engine with semi-GluC search parameter. The percolator node was used for false discovery rate (FDR) evaluation with a 5% filter in relaxed FDR and 1% in strict FDR. The Venny web resource was used to visualize peptides specific to the different conditions.

Evaluation of Mca1p Cleavage Specificity—Peptides identified by these analyses (native peptidomics and bottom-up digestions), at all FDR, were considered and only those exclusively present in the WT-farnesol condition with a Q-value under 0.05 were selected for further analysis. The "Extract Cleavage Site Context" algorithm in the Galaxy-P web resource (https://usegalaxyp.org/) was used to generate a list of sequences surrounding the cleavage sites of the peptides. The parameters used for this algorithm were: five amino acids at the N-terminal and C-terminal for the cleavage site context and a protease cleavage C-terminal to the cleavage site. All peptides with cleavage of initiation methionine only were eliminated. Cleavage specificities were represented by the Weblogo (http://weblogo.berkeley.edu/) (33) and Two Sample Logo algorithm with binomial test (http://www.twosamplelogo.org) (34). Extended cleavage specificities were investigated with IceLogo (https://code.google.com/p/icelogo/) (35) using the natural abundance of amino acids in the *C. albicans* protein sequence database (# 6209). For substrate validation, label-free approaches with Progenesis-LC software 4.1 (Nonlinear Dynamics Ltd, Newcastle, U.K.) of GluC and native peptidomics data sets were performed in a between-subject way. Potential substrates of Mca1p found on an identification basis were validated by considering those over-represented in WT-farnesol condition relative to the other conditions. Anova p-values under 0.05 calculated after label-free analysis of native peptidomics and GluC data sets were considered to select best potential substrates. A two factor analysis was performed to discriminate farnesol and/or mutation dependent or independent effects. GO analyzes were performed on the obtained list of potential substrates with the GO Slim Mapper tool of the *Candida* Genome Database website. P-values for functional enrichments were calculated with R 3.0.1 software for each GO term.

Data Availability—The complete sets of data are available as .raw files, Proteome Discoverer 1.4 .msf files and the *Candida albicans* protein sequence database provided as a multiple fasta in the Peptide Atlas repository under the identification number: PASS00561. The msf files can be visualized using a freely available java application Thermo-msf-parser 2.0.5 available at https://code.google.com/p/thermo-msf-parser/.

RESULTS

Mca1p is Required for Farnesol-induced Apoptosis in C. albicans—Farnesol, at the concentration and time of action chosen, had only a limited effect on the growth of the *mca1*Δ/Δ strain, although it slowed the growth of the wild-type strain. Annexin V-FITC and TUNEL labeling experiments showed that under these conditions, farnesol induced apoptosis in WT cells, but not in *mca1*Δ/Δ cells. Little or no specific fluorescence was detected in farnesol-treated *mca1*Δ/Δ cells, whereas more than 70% of the farnesol-treated WT cells were labeled (Fig. 1). No PI labeling was found in any of the four conditions indicating that the cells did not become necrotic. Consistent with this observation, the electrophoretic profile in SDS-PAGE experiments of total protein samples from the four conditions were very similar (supplemental Fig. S1). By comparing results between samples following these four experimental conditions, we investigated the role of the metacaspase Mca1p in the early phase of the apoptotic response in *C. albicans*.

Production of the Various Data Sets—Table I summarizes the results of the various analyses for protein (or peptide) content: trypsin digests, TMT-labeled samples, and GluC digests, all acquired in triplicates for each condition and the native peptidomic analyses run in duplicate for top-down evaluation of endogenous proteolysis in controls and farnesol-treated samples. The complete data sets are available in supplemental Data Files S1 to S5.

Evaluation of the Mca1p Cleavage Specificity—We used the Proteome Discoverer 1.4 software to determine changes to the peptide profile and abundance after GluC digestion, native peptidomic analyses, and trypsin digestion (Fig. 3; see supplemental Files S1, S2, and S4 for the complete data sets). The peptides found are represented in a Venn diagram according to the conditions (Fig. 3*A*). More peptides could be identified after Tryptic and GluC digests than native peptidomic analysis. Comparisons of protein profiles by SDS-PAGE indicated that farnesol and/or *mca1* disruption did not lead to any massive degradation of proteins (supplemental Fig. S1). We compared the cleavage site context for peptides found by native peptidomic analyses only in the WT-farnesol condition with those found only in the *mca1*Δ/Δ-farnesol condition. We examined the C-terminal residues of all the peptides identified in the top-down analyses, and we searched for partial cleavage specificity (semi-trypsin and semi-gluC) in the tryptic digests, where only K or R are expected except for the C-terminal fragment of the proteins, and in the GluC digests where an E, and to a lesser extent, a D are expected, except for the C-terminal fragment of the proteins. We expected to find enrichment in peptides with a D at the C-terminal end in the

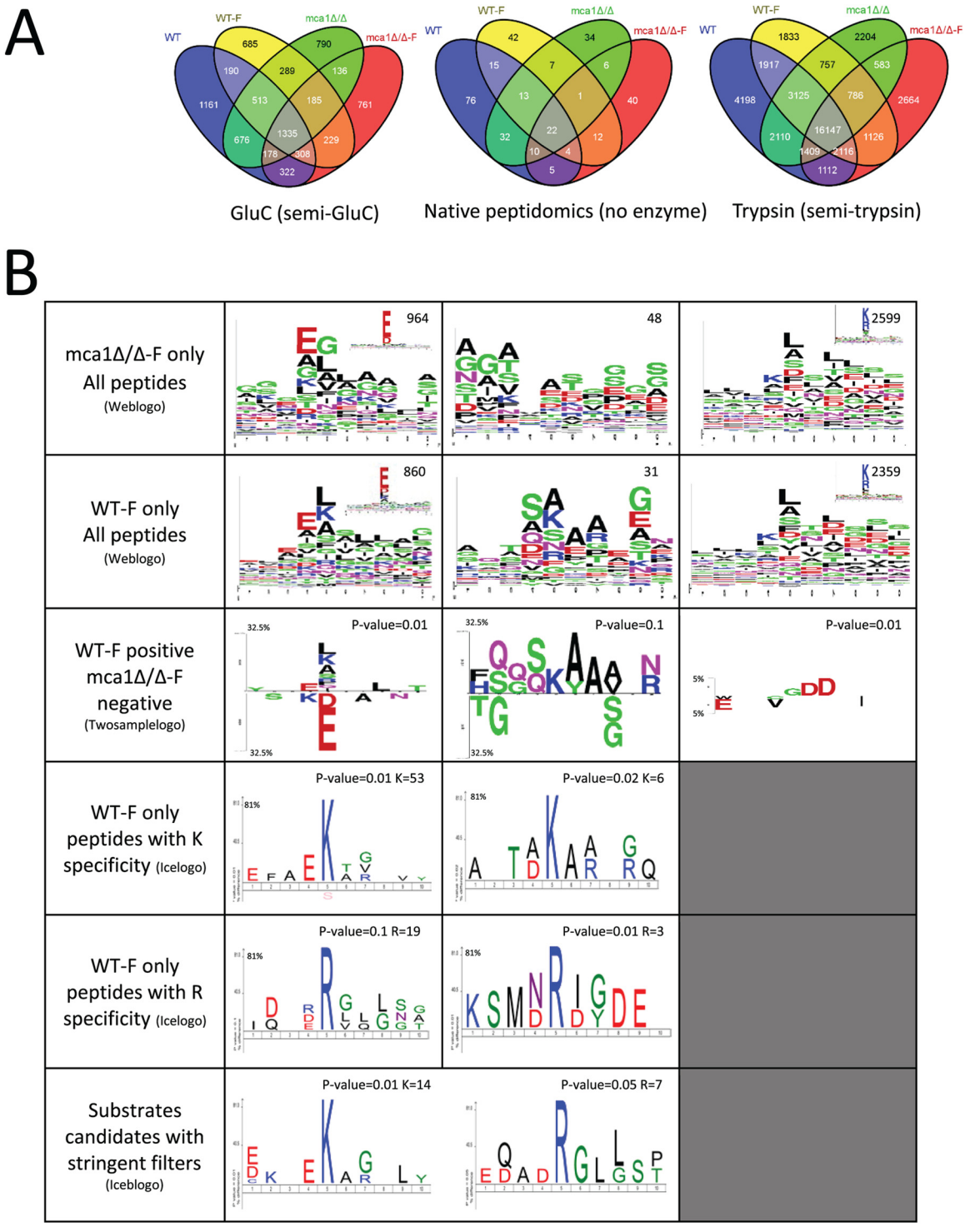

FIG. 3. **Evaluation of Mca1p cleavage specificity.** *A*, Venn diagrams showing the overlaps in differential peptide abundance in tryptic and GluC digests and native peptidomic analyses. *B*, Logo diagrams computed using the N-ter and C-ter extremities of peptides found only in WT-Farnesol and *mca1*Δ/Δ -farnesol conditions from the whole data sets produced in this study. Cleavage is considered at position five for all logos. Weblogo diagrams were used to visualize the general sequence context surrounding the cleavage site for all peptides (insets diagrams for GluC and trypsin experiments and diagrams for native peptidomic) and for peptides without D/E cleavage site (diagrams for GluC experiment) and without K/R (diagrams for trypsin experiment). The Two Sample Logo java applet was used to evaluate the cleavage specificity. Peptides found only in WT-farnesol are considered as the positive data set, whereas those found in *mca1*Δ/Δ -farnesol condition as the negative data set. A binomial test was used. IceLogo tool was used to determine extended cleavage specificities taking into account the natural abundance of amino-acids present in the *C. albicans* database used for all data sets.

TABLE II

Mca1p cleavage specificity. Occurrence of K/R residues in GluC and native peptidomic experiments according to the different strains used. The occurrence of D residue in tryptic digests (identified by semi-trypsin database search) is used as a control

Conditions	GluC	Native peptidomics	Trypsin
	K/R enrichment (%)	K/R enrichment (%)	D enrichment (%)
*mca1*Δ/Δ-F only	0.82	10.42	2.49
WT-F only	8.37	29.03	2.15
All conditions	3.84	20.18	1.70

TABLE III

Examples of Mca1p substrate candidates as identified by GluC and native peptidomic approaches. The peptides identified were present only in farnesol treated WT samples, with K or R extremities; they were found using a semi-gluC database search (the complete data set is provided as supplemental File S4 and the label-free quantitation as supplemental File S6) and a no-enzyme database search for native peptidomic experiment (the complete dataset is provided as supplemental File S2 and the label-free quantitation as supplemental File S7)

Accession	Description	Experiment	Sequences	Modification	Identification (2 replicates)		Label-free quantitation			
					Mascot score	q-value	Ratio WT-F/WT	Ratio WT-F/MCA1	Ratio WT-F/MCA1-F	Anova
orf19.778	PIL1 ORF|Verified, Eisosome component; predicted role in endocytosis; echinocandin-binding protein.	Native peptidomics	WGEDNEDDISDVTDK		48	0.012	7.8445	6.9551	5.7380	0.0002
orf19.7350	RCT1 Fluconazole-induced protein; elevated mRNA levels in a cyr1 or ras1 null mutant.	Native peptidomics	YDPKRSSNQGSSSSNDEQQDR		21,35	0	15.1728	Infinity	Infinity	0.0003
orf19.6754	ORF|Uncharacterized Protein of unknown function; Spider biofilm induced.	Native peptidomics	R.IGDEPVIRPVQT		32	0	9.6188	4.0665	12.2001	0.0072
Orf19.4309	GRP2 ORF|Verified "Methylglyoxal reductase; regulation associated with azole resistance; induced in core stress response or by oxidative stress via Cap1.	GluC	K.EKPNFTLSVINPVYVFGPQAFE		15	0.002	4.5502	1.4896	4.8340	0.0504174
Orf19.1896	TPI1 ORF|Verified Triose-phosphate isomerase; antigenic in mouse/human; mutation affects filamentation; possibly essential.	GluC	K.TRILYGGSVNGKNAKDFKDKANVD K.TRILYGGSVNGKNAKDFKDKANVD	N13(Deamidated)	16 18,13	0 0	3.6452 2.1933	2.3754 5.6150	6.5331 6.4354	0.104229 0.13929
orf19.2877	PIN3 ORF|Uncharacterized Putative SH3-domain-containing protein; predicted role in actin cytoskeleton organization.	GluC	K.TGVFPSNYVKIISQLE	N7(Deamidated); K10(Acetyl)	34	0.002	2.9009	1.5010	2.9144	0.03425641
Orf19.2340	CDC48 Putative microsomal ATPase; plasma membrane-localized.	GluC	R.FALGNSNPSALRE R.GQFSSFRFNE		54,36 35,31	0 0.005	2.1312 27.5506	2.8036 8.5435	2.5990 35.2983	0.016309 0.01541
orf19.2483	RIM1 ORF|Uncharacterized Putative single-stranded DNA-binding protein.	GluC	K.VGSLVHVD		40,48	0.001	12.3152	6.4978	5.6219	0.00047184
orf19.2644	QCR2 ORF|Verified Ubiquinol-cytochrome-c reductase; antigenic; induced by interaction with macrophage; repressed by nitric oxide.	GluC	R.GLGNPLFYNE		31	0.003	18.2867	32.0620	21.3631	0.0007934
orf19.1435	TEF1 ORF|Verified-Translation elongation factor 1-alpha; at cell surface.	GluC	HALLAYTLGVK K.SGKVTGKTLLE		11 28,18	0.031 0	4.3286 8.0996	4.6225 13.7924	20.2943 11.5797	0.044463 0.011313
orf19.6515	HSP90 Verified ORF; Essential chaperone, regulates several signal transduction pathways and temperature-induced morphogenesis; activated by heat shock, stress.	GluC	K.LVDAPAAIRTGQFGWSANME		23	0.007	4.0946	3.5352	9.6883	0.01435058
Orf19.6367	SSB1 Verified ORF; HSP70 family heat shock protein; possibly essential gene; sumoylation target.	GluC	R.LIGRAFDDE VSLLNITGGVFTVK		27,24 23	0.035 0.001	3.7434 -	5.1297 -	4.2345 -	0.00090087 -
orf19.4980	HSP70 Verified ORF; Putative hsp70 chaperone; role in entry into host cells; heat-shock, farnesol-downregulated in biofilm.	GluC	K.LVSDFFNGKE K.RTLSSSAQTSIE		19 27,12	0.041 0.041	2.7742 1.7147	3.8139 2.8943	1.7689 4.7633	4.45E-05 0.071418
orf19.3013	CDC12 ORF|Verified "Septin; essential for viability; forms ring at sites of cell division; regulated by cell density.	GluC	R.NRLNQDLEE		23	0.048	1.1990	2.0744	1.4868	0.08544746
orf19.2551	MET6 ORF|Verified "Essential 5-methyltetrahydropteroyltriglutamate-homocysteine methyltransferase (cobalamin-independent methionine synthase); heat shock.	GluC	K.ASAVVQKAIE		32	0.001	1.6794	3.5237	1.5264	0.13467686
orf19.1065	SSA2 Verified ORF; HSP70 family chaperone; farnesol-downregulated in biofilm.	GluC	K.RTLSSSAQTSIE R.LIGDAAKNQAAMNPANTVFD		27,12 20	0.041 0.02	1.7147 -	2.8943 -	4.7633 -	0.071418 -
Orf19.5928	RPP2B, translated using codon table 12 (111 amino acids) Verified ORF; Conserved acidic ribosomal protein, likely to be involved in regulation of translation elongation.	GluC	R.LQALLKDLE		33,42	0.001	Not quantified			

tryptic digest if Mca1p has the specificity of a caspase, or a K or R in GluC digests, if it does not. In wild-type cells where Mca1p is activated, we found a substantial enrichment in K and R cleavage sites in the semi-GluC database searches (Table III*B*). The comparison between peptides found in both *mca1*Δ/Δ and WT conditions with those observed in both farnesol conditions did not reveal any cleavage specificity for the trypsin digest other than the expected K/R residue in P1; this was consistent with the results from native peptidomic and GluC digest analyses. Calculated K/R enrichment of peptide ends for the different conditions confirmed the graphical visualization (Table II). Consideration of only those peptides with K/R ends is informative about the specificity of the protease Mca1p (Fig. 3*B*). Native peptidomic and GluC digest analyses showed that an acidic amino acid residue in P2 may be important for the cleavage specificity of Mca1p.

Native Peptidomic and GluC Digest Experiments to Identify Potential Mca1p Targets—GluC-directed bottom-up experiments identified 68 peptides (from 54 proteins) among a total of 8549 identified peptides (from 1261 proteins) as potential substrates of Mca1p. Native peptidomic analyses identified nine peptides (from eight proteins) among 416 (from 137 proteins) as potential substrates (supplemental Table S1). Substrate candidates were validated by a label-free approach on GluC digests and native peptidomics experiments (entire data sets in supplemental Files S6 and S7 respectively) with Progenesis-LC software. Peptides candidates (77 candidates) quantified (28 candidates) with higher abundances in WT-

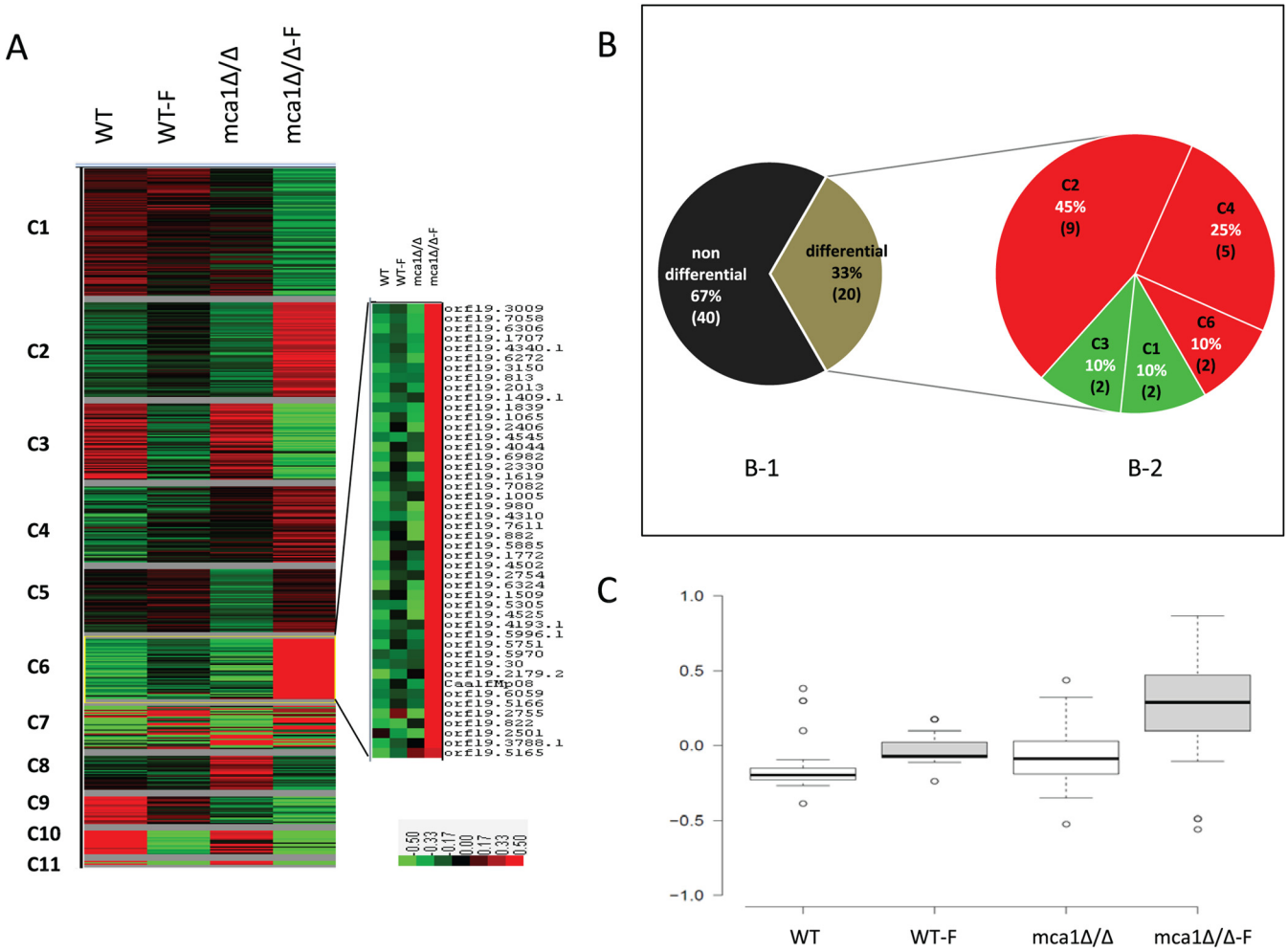

FIG. 4. **Classification of the proteins differentially expressed in the four experimental conditions.** *A*, Proteins for which the normalized abundance differed (ANOVA *p* value lower than 0.05) were sorted by the AutoClass Bayesian clustering system (webserver AutoClass@IJM, http://ytat2.ijm.univ-paris-diderot.fr/). All clusters and accessions are described in supplemental Fig. S2. *B*, Proteins candidate to be substrates of Mca1p found in native peptidomic and GluC digest experiments are distributed according to (*B*-1) their expression levels (black sector: no significant expression variation; green sector: significant variation in abundance) in label-free analyses of tryptic digests and to (*B*-2) their belonging to specific abundance profile clusters. *C*, Normalized abundance level of protein candidates to be substrates of Mca1p are represented in boxplot generated with BoxPlotR tool (http://boxplot.tyerslab.com/).

farnesol (23 candidates) than in the three other conditions and with an Anova p-value under 0.05 (13 candidates) were considered as best potential substrates. A p-value based on a two-way ANOVA was calculated to classify them and 12 reported an effect dependent of both strain and farnesol factors (supplemental Table S1). Table III provides examples of potential Mca1p substrates as found by native peptidomic or GluC digestion approaches, only in the WT-farnesol condition and with K or R ends.

Quantitative Assessment of Proteome Differences Between WT and mca1Δ/Δ in Response to Farnesol—We performed a label-free (Progenesis-LC) analysis of tryptic digests (four conditions, two replicates each) to investigate protein compositions: 2727 proteins were quantified with the parameter "trypsin for enzyme" and 503 proteins were thereby identified as differing between the conditions (differences of normalized abundance were significant with an ANOVA p-value lower than 0.05). The complete .htm files are supplied as supplemental File S5. We classified these differentially expressed proteins using the AutoClass@IJM Bayesian clustering system (32) (Fig. 4*A*). All clusters and accessions are presented in supplemental data (supplemental Table S2). The largest differences of protein abundance were between farnesol-treated and untreated cells, whether or not they carried the *MCA1* deletion. Most of the proteins that were more abundant in the WT-farnesol condition were also abundant in mca1Δ/Δ-farnesol extracts. We also ran independent analyses (in triplicate) of TMT-labeled digests. Quantifications of the reporter ions, and calculation of the abundance ratios confirmed the differences in protein abundance found in by label-free experiments. The TMT experiments allowed the identification of 1601 proteins with a 5% FDR threshold (see supplemental File

TABLE IV

Examples of differential protein expression as determined by label-free experiments. Differences in protein expression identified by label-free experiments with tryptic digests. All identified proteins and peptides are listed in supplemental Files S5 (.zip) and S8

Accession	Description	Wt	Wt-F	Mca1 -/-	Mca1 -/- F	Anova	Max fold	Protein score	Quantified Peptides	pValue_strain	pValue_farnesol	pValue_strain:farnesol
Orf19.4980	HSP70 Verified ORF; Putative hsp70 chaperone.					6.35e-003	2.00	1294.35	20	0.0217	0.0063	0.0314
Orf19.6515	HSP90 Verified ORF; Essential chaperone.					5.52e-004	2.13	3035.77	44	0.0022	0.0002	0.0006
Orf19.6387	HSP104 Verified ORF; Heat-shock protein.					3.28e-005	4.46	1772.50	36	0.0005	0.0004	0.0006
Orf19.882	HSP78 Uncharacterized ORF; Putative heat-shock protein.					2.61e-003	3.95	940.63	15	0.1185	0.0063	0.0298
Orf19.1065	SSA2 Verified ORF; HSP70 family chaperone, farnesol-downregulated in biofilm.					6.86e-004	3.06	1056.02	15	0.0007	0.0002	0.0010
Orf19.713	Uncharacterized ORF; Ortholog(s) have role in apoptotic process.					0.03	1.97	137.32	2	0.0284	0.06123	0.6098
Orf19.6312	RPS3 Uncharacterized ORF; Ribosomal protein S3; genes encoding cytoplasmic ribosomal subunits, translation factors, tRNA synthetases.					0.02	1.64	598	9	0.0569	0.0085	0.0154
Orf19.1896	SSC1 Verified ORF; Heat shock protein; at yeast-form cell surface, sumoylation target; possibly essential.					2.43e-003	1.65	2480	33	0.0230	0.0020	0.0683
Orf19.30	SPF1 Verified ORF; Putative calcium-transporting ATPase, response to ER stress.					0.01	2.11	304	6	0.0270	0.0348	0.0600
Orf19.5928	RPP2B Verified ORF; Conserved acidic ribosomal protein.					2.11e-003	1.92	113	1	0.0565	0.0011	0.0531
Orf19.2340	CDC48 Verified ORF; Putative microsomal ATPase; plasma membrane-localized.					4.09e-003	2.02	1211.46	19	0.0021	0.0015	0.0175
Orf19.506	YDJ1 Uncharacterized ORF; Putative type I HSP40 co-chaperone; heavy metal (cadmium) stress-induced.					7.39e-004	2.02	369.95	5	0.0298	0.0011	0.0024
Orf19.2175	Uncharacterized ORF; Putative mitochondrial cell death effector; induced by nitric oxide.					9.92e-004	4.23	220.59	4	0.0156	0.0014	0.0111
Orf19.6757	GCY1 Verified ORF; Possible aldo/keto reductase; farnesol-downregulated.					9.36e-003	1.74	754.14	9	0.4894	0.0019	0.02141
Orf19.2613	ECM4 Verified ORF; Cytoplasmic glutathione S-transferase; induced in core stress response.					3.18e-005	2.36	110.14	2	0.0069	3.616e-06	0.0004
Orf19.4082	DDR48 Verified ORF; Immunogenic stress-associated protein, farnesol, alkaline downregulated.					1.42e-004	12.86	4851.06	52	0.1190	0.0001	0.0051

S3 for the identified proteins). There was a very good correlation between the two quantification methods (supplemental Fig. S2). Scatter graphs of the ratios of protein abundances (WT-F/WT and *mca1*Δ/Δ-F/WT) indicated that proteins with the largest differences in abundance were common to the lists identified by both TMT labeling (supplemental Fig. S2*A*) and label-free (supplemental Fig. S2*B*) quantification analyses. Also, trend curves of the scatter graphs revealed that overall protein level in the farnesol condition was higher in mca1-disrupted than WT cells. Mca1p-specific peptides corresponding to the part of the gene deleted from the *mca1*Δ/Δ strain were found only in the wild-type extracts, and the abundance of Mca1p in the WT increased under farnesol treatment. However, Mca1p was not analyzed further because it was above the threshold in ANOVA (p-value of 0.06) and was not identified in TMT-labeling experiments. Label-free analyzes of tryptic digests indicated that 33% of proteins found to substrates of Mca1p were differentially expressed (80% being overexpressed) between *mca1*Δ/Δ-farnesol condition and the WT-farnesol condition (Fig 4*B*); this is significantly higher than the 18% of all proteins identified as being differentially expressed in label-free of tryptic digests. This is confirmed by a boxplot representation of potential substrates normalized abundances found in label-free of tryptic digests (Fig. 4*C*). Thus, not only were potential substrates degraded by Mca1p, but their production appears to be directly or indirectly inhibited by the protease.

Functional Analysis of Protein Variations Induced by Farnesol Treatment and/or mca1 Deletion—Representative examples of proteins the expression of which was affected by farnesol and/or the deletion of *MCA1* are presented in Table IV. The differences in abundance were measured by a label-free approach with trypsin digests and confirmed by a TMT-labeling approach (Table V). Some of the potential substrates for Mca1p, including chaperone proteins Hsp70p, Hsp90p, and Ssb1p were found differentially expressed in label-free and TMT-labeling analyses of tryptic digests. Gene ontology analyses of the potential substrates of Mca1p confirmed a significant enrichment in proteins implicated in the stress response and folding (supplemental Table S3). Several targets, such as Hsp90p, Rps3p, and Cdc48p, were predicted to interact with Mca1p in *C. albicans* (excepted for the last

TABLE V

Examples of differential protein expression analysis by the TMT-labeling approach. Proteins expressed differently in different samples were identified by TMT-labeling experiments. All identified proteins and peptides are listed in supplemental File S3. 126, 127, 128 and 129 labeling represents respectively WT, WT-farnesol, mca1Δ/Δ and mca1Δ/Δ-farnesol conditions

Accession	Description	127/126 (variability %)	128/126 (variability %)	129/126 (variability %)	Protein score	Quantified peptides
Orf19.4980	HSP70 Verified ORF; Putative hsp70 chaperone; role in entry into host cells; heat-shock, amphotericin B, cadmium, ketoconazole-ind	1.438 (3.0)	0.972 (0.9)	2.034 (3.5)	1426	11
Orf19.6515	HSP90 Verified ORF; Essential chaperone, regulates several signal transduction pathways and temperature-induced morphogenesis	1.206 (2.4)	0.814 (2.3)	1.942 (2.9)	1180	35
Orf19.6387	HSP104 Verified ORF; Heat-shock protein; roles in biofilm and virulence; complements chaperone and prion propagation activity in S	1.355 (2.6)	0.913 (2.9)	4.252 (9.4)	903	31
Orf19.882	HSP78 Uncharacterized ORF; Putative heat-shock protein; transcriptionally regulated by macrophage response; transcription is regulated by Nrg1p, Mig1p, Gcn2p, Gcn4p, Mnl1p; heavy metal (cadmium) stress-induced; stationary phase enriched protein	1.750 (8.9)	0.877 (1.8)	3.268 (20.0)	162	12
Orf19.1065	SSA2, translated using codon table 12 (645 amino acids) Verified ORF; HSP70 family chaperone; found in cell wall fractions; antigenic; role in import of beta-defensin peptides; ATPase domain binds histatin 5; at surface of hyphae, not yeast-form cells; farnesol-downregulated in biofilm;	1.295 (1.5)	0.790 (0.7)	2.049 (2.0)	1445	14
Orf19.2013	KAR2, translated using codon table 12 (687 amino acids) Verified ORF; Similar to chaperones of Hsp70p family; role in translocation of proteins into the ER; transcriptionally regulated by iron; expression greater in high iron; protein present in exponential and stationary growth phase yeast cultures	1.393 (1.8)	0.847 (1.9)	2.129 (2.9)	860	24
Orf19.2175	Uncharacterized ORF; Putative mitochondrial cell death effector; induced by nitric oxide	1.7 (20.4)	0.885 (4.4)	1.506 (12.3)	41	3
Orf19.6541	RPL5, translated using codon table 12 (298 amino acids) Uncharacterized ORF; Ribosomal protein; genes encoding cytoplasmic ribosomal subunits, translation factors, tRNA synthetases are downregulated upon phagocytosis by murine macrophages; Hap43p-induced gene	1.303 (8.1)	0.832 (2.9)	1.662 (4.6)	280	8
Orf19.6059	TTR1, translated using codon table 12 (119 amino acids) Verified ORF; Putative glutaredoxin; described as a glutathione reductase; upregulated in the presence of human neutrophils, and upon benomyl treatment; alkaline downregulated; regulated by Gcn2p and Gcn4p; required for virulence in mouse model	1.199 (5.1)	0.901 (4.3)	1.737 (2.9)	71	5
Orf19.4082	DDR48 Verified ORF; Immunogenic stress-associated protein; regulated by filamentous growth pathways; induced by benomyl, caspofungin, ketoconazole or in azole-resistant strain; Hog1p, farnesol, alkaline downregulated; stationary phase enriched; biofilm-induced	0.485 (5.3)	1.191 (0.7)	0.303 (40.4)	423	11
orf19.1760	RAS1, translated using codon table 12 (291 amino acids) Verified ORF; RAS signal transduction GTPase; regulates cAMP and MAP kinase pathways; role in hyphal induction, virulence, apoptosis, heat-shock sensitivity; nonessential; plasma membrane-localized; complements viability of S. cerevisiae ras1 ras2 mutant	0.989 (5.8)	0.886 (6.6)	1.016 (5.9)	153	6
orf19.6000	CDR1, translated using codon table 12 (1501 amino acids) Verified ORF; Multidrug transporter of ATP-binding cassette (ABC) superfamily; transports phospholipids in an in-to-out direction; transcription induced by beta-estradiol, progesterone, corticosteroid, or cholesterol; repressed in young biofilms	2.991 (21.5)	0.846 (2.1)	2.692 (16.4)	130	8
orf19.6312	RPS3, translated using codon table 12 (251 amino acids) Uncharacterized ORF; Ribosomal protein S3; Hog1p-, Hap43p-induced; genes encoding cytoplasmic ribosomal subunits, translation factors, tRNA synthetases are downregulated upon phagocytosis by murine macrophage; present in exponential and stationary phase cells	1.199 (1.6)	0.799 (2.6)	1.534 (2.7)	210	11
Orf19.5928	RPP2B Verified ORF; Conserved acidic ribosomal protein, likely to be involved in regulation of translation elongation; interacts with Rpp1Ap; one of four similar C. albicans ribosomal proteins (Rpp1Ap, Rpp1Bp, Rpp2Ap, Rpp2Bp); macrophage/pseudohyphal-induced	1.342 (4.2)	0.829 (3.7)	1.712 (4)	98	1
Orf19.7085	Uncharacterized ORF; Predicted ORF in Assemblies 19, 20 and 21; induced in core stress response; induced by heavy metal (cadmium) stress via Hog1p; oxidative stress-induced via Cap1p; induced by Mnl1p under weak acid stress; macrophage-downregulated	1.868 (3.1)	0.939 (6.9)	10.903 (9.3)	193	11
Orf19.2340	CDC48 Verified ORF; Putative microsomal ATPase; plasma membrane-localized; regulated by Gcn2p and Gcn4p; induced by amino acid starvation (3-AT treatment); macrophage/pseudohyphal-repressed; protein levels decrease in stationary phase yeast cultures	1.241 (1.8)	0.894 (2.3)	1.689 (4.8)	889	31
Orf19.506	YDJ1 Uncharacterized ORF; Putative type I HSP40 co-chaperone; heavy metal (cadmium) stress-induced	1.187 (5.1)	0.858 (2.2)	1.553 (2.3)	149	7

protein: just in *S. cerevisiae*) by the String 9.0 web resource (Fig. 5). Gene ontology analyses also revealed that many of the potential substrates found by GluC experiments are mitochondrial proteins (*e.g.* Qcr2p, Rim1p, Pil1p, Tpi1p, Rct1p, and Atp5p) or associated with the plasma membrane or the cell wall, or are extracellular (supplemental Table S3). Some potential substrates are involved in carbohydrate metabolism and in the generation of precursor metabolites and energy, functions associated with mitochondria and glycolysis (Tpi1p, Fba1p, and Gpm1p).

Farnesol increased the abundance of heat shock proteins (Hsp70p, Hsp90p, Hsp104p, Ssc1p, and Kar2p for example) in the WT, with the effect being much larger in the mca1-deleted strain (Tables IV and V). The level of a putative mitochondrial cell death effector (orf19.2175), an ortholog of Aif1p in *S. cerevisiae*, was increased by farnesol in the WT and to a lesser extent in the mutant (Table IV). Ras1p, a protein involved in apoptosis through the RAS1/cAMP/PKA pathway in *C. albicans* (36), did not differ between any of the conditions analyzed. The abundance of Tpk2p, a catalytic subunit of PKA, was higher in WT-farnesol cells than in *mca1*Δ/Δ cells in the presence of farnesol (supplemental File S5).

We performed a gene ontology analysis on the various classes of proteins with similar abundance profiles (Autoclass clusters) that allowed us to evaluate the effect of farnesol and Mca1p on the "cellular component," the "biological process," and the "molecular function" terms. A Mca1p-dependent effect of farnesol was clearly demonstrated for a number of proteins involved in carbohydrate metabolism. However, the abundance of numerous proteins was not dependent on the presence of the Mca1p protease. The level of proteins involved in the response to oxidative stress increased with farnesol and was higher in the absence of Mca1p in the farnesol condition. The abundance of proteins implicated in processes such as "translation," "ribosome biogenesis," and "protein folding" in the presence of farnesol was still higher in the *mca1*Δ/Δ than WT strain (supplemental Table S4). The same was found by analysis of the "structural activity" and "RNA binding" terms of "molecular function" entries (supplemental Table S4). Differences in the control of translation between farnesol-treated *mca1*Δ/Δ and farnesol-treated WT cells were confirmed by the overexpression of proteins in the nucleolus observed in extracts. Expression of some Mca1p partners predicted by the String 9.0 database web resource

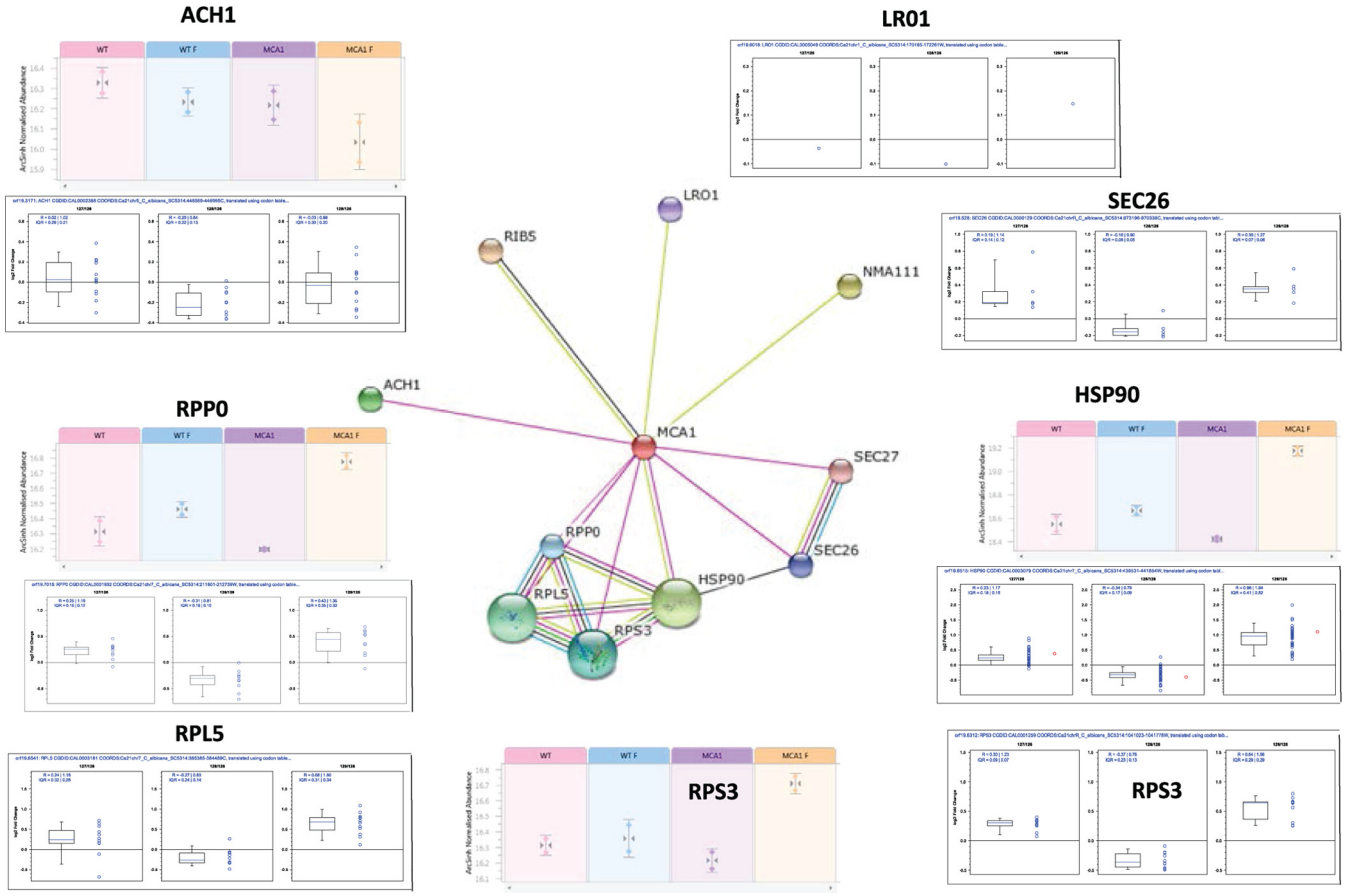

FIG. 5. **Expression levels of predicted partners of mca1p (central panel from string 9.0 website).** Corresponding abundances of these proteins as determined by TMT experiments are shown with WT-F/WT, *mca1*Δ/Δ/WT, and *mca1*Δ/Δ-F/WT ratios and as determined by label-free experiments with WT, WT-F, *mca1*Δ/Δ, and *mca1*Δ/Δ-F abundance.

(http://string-db.org/) was increased by farnesol and was higher in the Mca1p-deleted than WT strains (Fig. 5).

Farnesol Induces Cdr1p Overexpression and its Glutathionylation in a Mca1p-Independent Way—Label-free analysis of tryptic digests and TMT-labeling experiments showed that farnesol increased the abundance of Cdr1p, an ABC multidrug transporter, in a Mca1p-independent way (Fig. 6*A*). Cdr1p has been described as exporting glutathione from farnesol-treated cells, so we searched for signatures of this activity in our data. A database search of tryptic digests for the post-translational modification glutathionylation (C) revealed no overall difference (Q-value threshold at 0.05) in the glutathionylated proteomes in the different conditions (Fig. 6*C*). We found that Cdr1p itself was glutathionylated on cysteine 712 (Fig. 6*B*) in the WT and the *mca1*Δ/Δ extracts prepared after farnesol treatment. No differences in reduced glutathione between the different conditions was found by flow cytometry and naphthalene-2,3-dicarboxaldehyde labeling (Fig. 6*D*).

Western blot Analyses of a Putative Substrate of Mca1p—Immunoblot with anti-Ssb1p antibody confirmed abundances variation found for this protein in label-free experiment of tryptic digests (Fig. 7). We showed a higher Ssb1p abundance in *mca1*Δ/Δ-farnesol condition relative to other conditions. Moreover, a fragment of this protein was detected (around 20 kDa) only in WT-farnesol condition indicating that the Ssb1p cleavage is caused by the activated Mca1p protease as shown in GluC digest bottom-up approach (Table III).

DISCUSSION

When analyzing the *C. albicans* metacaspase function, we wondered whether it is possible to address its endopeptidase activity from *in vivo* experiments. Therefore, we conducted a series of proteomic studies to: (1) evaluate the role of Mca1p in the early phase of apoptosis in *C. albicans*, (2) investigate the proteolytic activity of Mca1p and determine whether it is a general purpose protease, or an enzyme with specific substrates, and (3) decipher the cleavage specificity of Mca1p. We analyzed, in parallel, the proteomes of two *C. albicans* strains, a wild-type strain and an isogenic strain from which both alleles of the *MCA1* gene were deleted, grown under non-filamentous conditions (yeast form) in the presence and absence of a low concentration of the apoptosis inducer farnesol. This allowed analysis of the events during an early

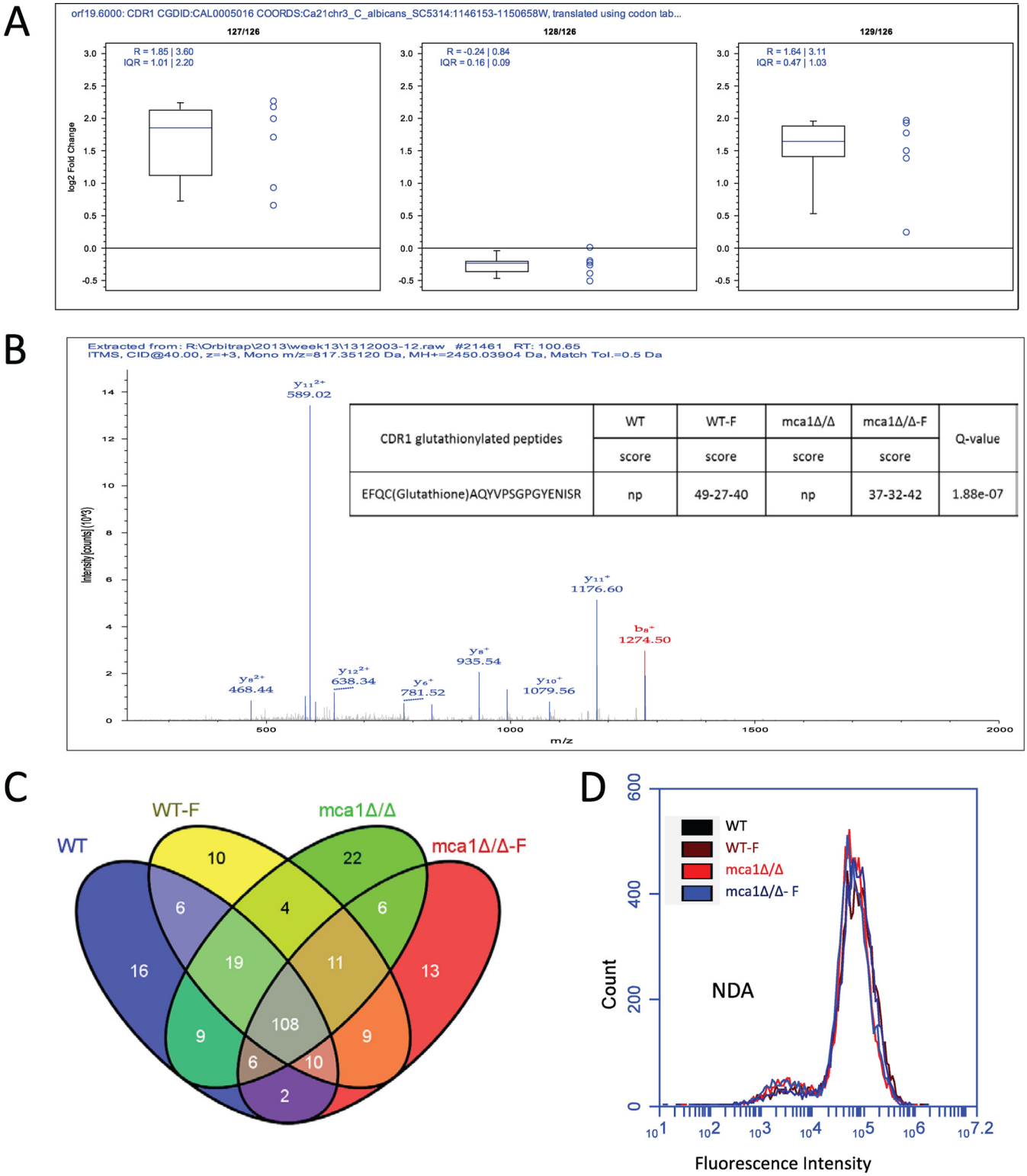

CDR1 glutathionylated peptides	WT	WT-F	mca1Δ/Δ	mca1Δ/Δ-F	Q-value
	score	score	score	score	
EFQC(Glutathione)AQYVPSGPGYENISR	np	49-27-40	np	37-32-42	1.88e-07

FIG. 6. **Case study of Cdr1p expression and post-translational modification.** *A*, TMT-labeling experiment shows that Cdr1p expression is increased by farnesol in a Mca1p-independent way. *B*, Details of glutathionylated peptide identified in trypsin digests and found only in the three replicates of farnesol-treated samples. Spectrum of the glutathionylated peptide. *C,* Venn representation of glutathionylated proteins identified in tryptic digests with a 5% FDR threshold. *D,* Measurement of reduced glutathione by flow cytometry with NDA labeling.

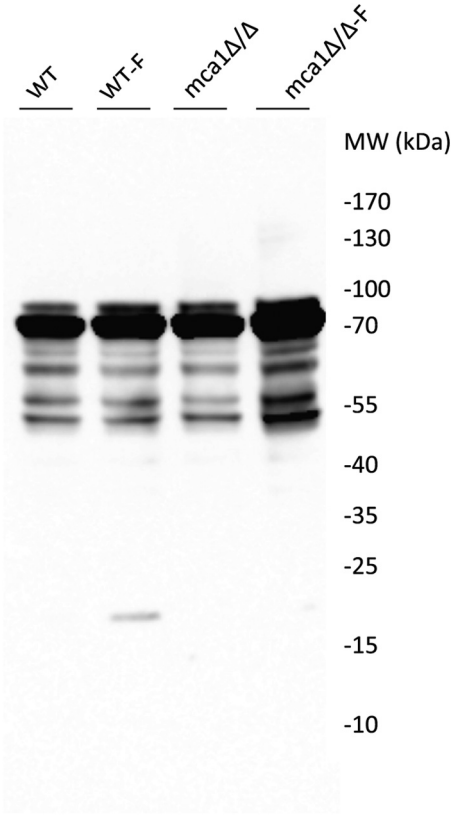

FIG. 7. **Western blot analyses of a putative substrate of Mca1p.** Visualization of Ssb1p abundance by immunoblot in WT, WT-farnesol, *mca1*Δ/Δ, and *mca1*Δ/Δ-farnesol conditions. Control immunoblot without primary antibody gave no signal (data not shown).

phase of apoptosis, before the massive degradation events lea ding to necrosis. The action of farnesol action is dependent on Mca1p expression (10). Under the experimental conditions used (250 μM farnesol applied for 4h to yeast cells in the mid log phase of growth), there was a clear difference in biological responses between the WT and the *mca1*Δ/Δ strains. In the WT cells but not in the *mca1*Δ/Δ cells farnesol induced the externalization of phosphatidyl serine and some fragmentation of nuclear DNA indicating apoptosis. However, none of the cells were significantly labeled with propidium iodide, indicating that they were not necrotic. These observations confirmed that the presence of an active metacaspase is required for *C. albicans* programmed cell death. Most studied caspases have a relatively strict specificity for an aspartic acid residue (D) in P1 (6, 7) whereas several metacaspases from plants, yeasts or some metazoans tend to be specific for basic residues (K/R) (7, 37, 38). The clear enrichment in K/R cleavage sites we found for Mca1p indicates a cleavage specificity similar to that described for several fungal metacaspases (as determined using synthetic peptides) including the *Allomyces arbuscula* metacaspase CDPII (37) and Yca1p in *S. cerevisiae* (25, 38); this is also the specificity displayed by plant metacaspases 4 and 9 in *Arabidopsis thaliana* (7), or mcII-PA in the Norway spruce tree (39). There were only a small number of peptides fulfilling our selection criteria in the various conditions and no cleavage specificity other than a K/R residue was found by comparison of WT-farnesol and *mca1*Δ/Δ-farnesol using native peptidomic analyses, or gluC and trypsin digests. This indicates that the apoptosis events analyzed did not result from a massive and nonselective degradation of cellular protein. Mca1p appears to be specific to a limited number of substrates, and does not seem significantly to activate other proteases. Moreover, our results showed an interesting bias with over-representation of an acidic residue (D or E) in the P2 position relative to the cleavage site. An acidic D/E predominance at P1′ and to a lower extent at P2 has been described for the metacaspase 9 in *A. thaliana* (40) and a basic residue (K or R) at P2 inhibits totally the activity of the CDPII metacaspase of *Allomyces arbuscula* (37). Overall, we report 54 proteins (77 peptides) as potential substrates of Mca1p *in vivo* during the early phase of farnesol-induced apoptosis in the yeast form of *C. albicans*. Among these 77 peptides at least 13 were considered as the best substrates candidates (supplemental Table S1) with more drastic filters. One of the most striking features of the specificity of Mca1p is that many of these substrates belong to either the family of heat-shock proteins (Ssb1p, Hsp70p, and Hsp90p), and translation machinery (Tef1p, Rps3p, Rpl17Bp, Rpp2Bp, and Hcr1p), or to mitochondria (Qcr2p, Aco1p, Cox5p, and Atp5p) and carbon metabolism (Tpi2p, Tal1p, Tkl1p, Gpm1p, Fba1p, Lsc1p, Lpd1p, and Pmm1p). We confirmed by immunoblot the cleavage of Ssb1p, an HSP family heat-shock protein, in the experimental condition where the metacaspase is activated. This suggests that the onset of apoptosis is associated with a loss of general stress response capabilities and a major metabolic rewiring.

Our quantitative proteomic experiments clearly show that diverse biological responses are elicited by farnesol treatment. Some are Mca1p-dependent, others are Mca1p-independent. Also, the proteome differs according to the presence/absence of Mca1p without farnesol treatment. One purely farnesol effect was the strong induction of Cdr1p, a plasma membrane associated ABC transporter and that has been linked to farnesol toxicity (18, 41). Cdr1p mediates the extrusion of glutathione from farnesol-treated cells, leading to a depletion of the intracellular pools of GSH, and therefore enhanced susceptibility to oxidative stress (41). We examined differences between the glutathionylated proteomes in the various bottom-up data sets to study the role of Cdr1p in our experimental model of farnesol-induced apoptosis. There were no massive differences in overall protein glutathionylation, with a core of 108 proteins remaining glutathionylated in all conditions. This does not reflect the expected effects of massive glutathione extrusion triggered by farnesol. This observation was confirmed by an evaluation of the cellular content of reduced glutathione by measuring the formation of a fluorescent adduct with naphthalene-2,3-dicarboxaldehyde (30) and flow cytometry analysis: no significant differences

were detected between the GSH pools in the different conditions assayed. There were however some specific targets of protein glutathionylation upon farnesol treatment, and in particular, the presence of farnesol led to Cys712 of Cdr1p being glutathionylated irrespective of the presence or absence of Mca1p. This cysteine residue is located in a transmembrane helix (TM4), and a mutational analysis did not find that it has any critical function in the transport activity of Cdr1p (42). The role of Cdr1p glutathionylation remains unclear. The crystal structures of two ABC transporters in the presence of glutathione, the mitochondrial iron–sulfur cluster exporter Atm1p from *S. cerevisiae* and the heavy metal Atm1-type ABC exporter from *Novosphingobium aromaticivorans (*43, 44), may provide some clues. Others proteins, such as Hsp104p, were glutathionylated (on Cys544 and Cys640) in farnesol-treated samples but only when Mca1p was absent.

We defined clusters of proteins with similar expression profiles across the different experimental conditions, as determined by the quantitative label-free and the TMT-labeling analyses. The resulting protein classes (Fig. 5) revealed some characteristic expression profiles. Clusters C3 and C10 contain proteins the expression of which was lowered by farnesol treatment independently of the presence of Mca1p; clusters C2 and C10, and to a lesser extent C4, include proteins showing a much larger increase in protein abundance upon farnesol treatment when Mca1p is absent than in wild-type cells. Statistical analysis of the enrichment of gene ontology terms (cellular component, biological process, and molecular function) in the various clusters indicated that the main processes altered are related to stress response, and ribosome biogenesis, protein translation and folding. Farnesol increases the expression of proteins involved in folding and response to stress such as Hsp90p, Ssa1p, Hsp60p, and Glr1p (10). Here, we show that the mca1 deletion considerably enhances the induction of these proteins, but also the induction of other chaperones including Hsp104p, Ssc1p, Ddr48p, and orf19. 7085p. This result raises important questions about the molecular function of Mca1p. Some phenotypes of *mca1*-deleted *C. albicans* strains have been described (22): the absence of Mca1p leads to elevated resistance of the cells to oxidative stress, alteration of mitochondrial energy production and rerouting of glucose metabolism. Resistance to oxidative stress is also increased by the down-regulation of the RAS1/cAMP/PKA pathway by farnesol in *C. albicans*. This pathway accelerates PCD by inhibiting the expression of stress proteins or by inducing factors of apoptosis (36). Although we did not observe any effects on Ras1p expression, farnesol increased the expression of Tpk2p, a catalytic subunit of PKA, but this effect was not observed in the Mca1p mutant. This is coherent with the HSP-related phenotypes of the *mca1*Δ/Δ cells in the presence of farnesol, but cannot be traced back to a PKA-dependent inhibition of the expression of the catalase Cat1p, a major contributor to farnesol-induced oxidative stress (15). The differences in expression of Tpk2p are corroborated by those observed for the apoptosis-inducing factor Aif1p ortholog, in our label-free experiments (Table I). Possibly, the RAS1/cAMP/PKA pathway increases the expression of Aif1p ortholog to induce apoptosis events, and this activation may be dependent on the presence of Mca1p.

The sequences and structures of Mca1p in *C. albicans* and the *S. cerevisiae* ortholog of Mca1p, the metacaspase Yca1p are very similar, so they are likely to share various functions. An important function of Yca1p is its contribution to the clearance of aggregated proteins in stressed cells (23, 24). Yca1p has been found associated with aggregated proteins, together with Cdc48p, a member of the HSP family, and with the aggregate-remodeling chaperones Ssa1p and Ssa2p (24). It has been suggested that mechanism of action of Yca1p is bind to insoluble aggregated proteins and then recruit unfolding/degradation machinery to eliminate them. Our results suggest that Mca1p functions differently: the protein chaperones, including Hsp104p, a major disaggregase in *C. albicans* (45) appear to be the substrates of Mca1p. The main function of Mca1p appears therefore to be to reduce the capacity of stressed cells to respond to protein alterations, thereby favoring cell death.

Our analyses suggest a second important function of Mca1p. A number of mitochondrial proteins appear to be direct (Cox1p, Atp5p) or indirect (Aif1p) substrates for Mca1p; proteolytic cascades and degradation of mitochondrion are major events of apoptosis (10, 46, 47), so this reveals a link between Mca1p-dependent apoptosis and the mitochondrial pathway for PCD. Mutations in Cdc48p in *S. cerevisiae* result in mitochondrion impairments and apoptosis (48). Here, we show that Cdc48p is a potential substrate of Mca1p, with three cleavage sites found, two of which found with the most stringent filters applied. This suggests thus that the endopeptidase activity of Mca1p may directly degrade or at least impair mitochondria. This is relevant to a previously unexplained observation that deleting YCA1 from a frataxin-deficient *yfh1*Δ strain that exhibits severe mitochondrial dysfunctions, allows the restoration of cytochromes assembly (49). *YCA1* deletion may lower the rate of mitochondria degradation and thereby allow the synthesis and maintenance of partly functional mitochondria. The deletion of *MCA1* in *C. albicans* results in a lower abundance of ROS and a lower mitochondrial membrane potential (22). We report here that the expression of a putative effector of death (orf19.2175), ortholog of the *S. cerevisiae* Aif1p described to be a mitochondrial apoptosis effector (50), is increased by farnesol in the WT and by less in the *mca1*Δ/Δ mutant. Differences in the expression of the apoptosis effector are corroborated by flow cytometric analysis of the activation of apoptosis. However, the expression of this apoptosis inducer in the presence of farnesol was high even in the *mca1*Δ/Δ strain, higher than would be expected in the light of the flow cytometry results. This suggests that the induction of apoptosis by the Alf1p

ortholog is mostly dependent of Mca1p, consistent with what has been described in *S. cerevisiae* (50).

Native peptidomic analyses identified only 9 of 416 peptides as potential substrates of Mca1p, and GluC experiments found only 68 among 8549 peptides. This suggests that the metacaspase has a targeted activity. Here, we show that the endopeptidase activity of Mca1p is tightly targeted and directed toward mitochondria, chaperone proteins, and glycolysis proteins, causing mitochondrial damage and thus apoptosis. It would be interesting to investigate the contribution, if any, of cytoplasmic proteases including Mca1p in proteasome and vacuole degradation during apoptosis. No quantitative differences in the numbers of ubiquitinated species were found in our proteomic analyzes of whole protein extracts according to the presence or absence of farnesol and/or Mca1p disruption (data not shown).

In conclusion, the results presented help elucidate the possible functions of Mca1p in *C. albicans*. Mca1p appears to act as a specific protease, with a limited number of substrates. Another function of Mca1p is to reduce the capability of the cells to respond to stress, by degrading key components of the protein chaperone machineries. Also, Mca1p contributes significantly to the control of mitochondrial biogenesis and degradation, and thereby probably constituting a link between the extrinsic and the intrinsic programmed cell death pathways in *C. albicans*. Mca1p function could be further described by studying the kinetics of apoptotic responses using a combination of apoptosis inducers.

Acknowledgments—We thank Dr Véronique Albanese, IJM, Paris, for the generous gift of the anti-Ssb1 antibody. Camille Garcia was the recipient of a grant-in-aid from the CNRS. We thank Alex Edelman & Associates for the edition of the English text.

Ⓢ This article contains supplemental Figs. S1 and S2, Tables S1 to S4, and Files S1 to S9.

¶ To whom correspondence should be addressed: Department of Proteomics, Institut Jacques Monod, CNRS Univ Paris Diderot, 15 Rue Helene Brion, Paris 75013, France. Tel.: 33-01-57278029; E-mail: camadro.jean-michel@ijm.univ-paris-diderot.fr.

REFERENCES

1. Tait, S. W., and Green, D. R. (2010) Mitochondria and cell death: outer membrane permeabilization and beyond. *Nat. Rev. Mol. Cell Biol.* **11,** 621–632
2. Brunelle, J. K., and Letai, A. (2009) Control of mitochondrial apoptosis by the Bcl-2 family. *J. Cell Sci.* **122,** 437–441
3. Bratton, S. B., and Salvesen, G. S. (2010) Regulation of the Apaf-1-caspase-9 apoptosome. *J. Cell Sci.* **123,** 3209–3214
4. Shi, Y. (2002) Mechanisms of caspase activation and inhibition during apoptosis. *Mol. Cell* **9,** 459–470
5. Boatright, K. M., and Salvesen, G. S. (2003) Mechanisms of caspase activation. *Curr. Opin. Cell Biol.* **15,** 725–731
6. Thornberry, N. A., Rano, T. A., Peterson, E. P., Rasper, D. M., Timkey, T., Garcia-Calvo, M., Houtzager, V. M., Nordstrom, P. A., Roy, S., Vaillancourt, J. P., Chapman, K. T., and Nicholson, D. W. (1997) A combinatorial approach defines specificities of members of the caspase family and granzyme B. Functional relationships established for key mediators of apoptosis. *J. Biol. Chem.* **272,** 17907–17911
7. Vercammen, D., van de Cotte, B., De Jaeger, G., Eeckhout, D., Casteels, P., Vandepoele, K., Vandenberghe, I., Van Beeumen, J., Inze, D., and Van Breusegem, F. (2004) Type II metacaspases Atmc4 and Atmc9 of Arabidopsis thaliana cleave substrates after arginine and lysine. *J. Biol. Chem.* **279,** 45329–45336
8. Carmona-Gutierrez, D., Eisenberg, T., Buttner, S., Meisinger, C., Kroemer, G., and Madeo, F. (2010) Apoptosis in yeast: triggers, pathways, subroutines. *Cell Death Differ.* **17,** 763–773
9. Madeo, F., Frohlich, E., and Frohlich, K. U. (1997) A yeast mutant showing diagnostic markers of early and late apoptosis. *J. Cell Biol.* **139,** 729–734
10. Shirtliff, M. E., Krom, B. P., Meijering, R. A., Peters, B. M., Zhu, J., Scheper, M. A., Harris, M. L., and Jabra-Rizk, M. A. (2009) Farnesol-induced apoptosis in Candida albicans. *Antimicrob. Agents Chemother.* **53,** 2392–2401
11. Cao, Y. Y., Cao, Y. B., Xu, Z., Ying, K., Li, Y., Xie, Y., Zhu, Z. Y., Chen, W. S., and Jiang, Y. Y. (2005) cDNA microarray analysis of differential gene expression in Candida albicans biofilm exposed to farnesol. *Antimicrob. Agents Chemother.* **49,** 584–589
12. Hornby, J. M., Jensen, E. C., Lisec, A. D., Tasto, J. J., Jahnke, B., Shoemaker, R., Dussault, P., and Nickerson, K. W. (2001) Quorum sensing in the dimorphic fungus Candida albicans is mediated by farnesol. *Appl. Environ. Microbiol.* **67,** 2982–2992
13. Sato, T., Watanabe, T., Mikami, T., and Matsumoto, T. (2004) Farnesol, a morphogenetic autoregulatory substance in the dimorphic fungus Candida albicans, inhibits hyphae growth through suppression of a mitogen-activated protein kinase cascade. *Biol. Pharm. Bull.* **27,** 751–752
14. Jabra-Rizk, M. A., Shirtliff, M., James, C., and Meiller, T. (2006) Effect of farnesol on Candida dubliniensis biofilm formation and fluconazole resistance. *FEMS Yeast Res.* **6,** 1063–1073
15. Deveau, A., Piispanen, A. E., Jackson, A. A., and Hogan, D. A. (2010) Farnesol induces hydrogen peroxide resistance in Candida albicans yeast by inhibiting the Ras-cyclic AMP signaling pathway. *Eukaryotic Cell* **9,** 569–577
16. Langford, M. L., Hargarten, J. C., Patefield, K. D., Marta, E., Blankenship, J. R., Fanning, S., Nickerson, K. W., and Atkin, A. L. (2013) Candida albicans Czf1 and Efg1 coordinate the response to farnesol during quorum sensing, white-opaque thermal dimorphism, and cell death. *Eukaryotic Cell* **12,** 1281–1292
17. Dai, B., Wang, Y., Li, D., Xu, Y., Liang, R., Zhao, L., Cao, Y., Jia, J., and Jiang, Y. (2012) Hsp90 is involved in apoptosis of Candida albicans by regulating the calcineurin-caspase apoptotic pathway. *PloS One* **7,** e45109
18. Sharma, M., and Prasad, R. (2011) The quorum-sensing molecule farnesol is a modulator of drug efflux mediated by ABC multidrug transporters and synergizes with drugs in Candida albicans. *Antimicrob. Agents Chemother.* **55,** 4834–4843
19. Bozhkov, P. V., Suarez, M. F., Filonova, L. H., Daniel, G., Zamyatnin, A. A., Jr., Rodriguez-Nieto, S., Zhivotovsky, B., and Smertenko, A. (2005) Cysteine protease mcII-Pa executes programmed cell death during plant embryogenesis. *Proc. Natl. Acad. Sci. U.S.A.* **102,** 14463–14468
20. Madeo, F., Herker, E., Maldener, C., Wissing, S., Lachelt, S., Herlan, M., Fehr, M., Lauber, K., Sigrist, S. J., Wesselborg, S., and Frohlich, K. U. (2002) A caspase-related protease regulates apoptosis in yeast. *Mol. Cell* **9,** 911–917
21. Khan, M. A., Chock, P. B., and Stadtman, E. R. (2005) Knockout of caspase-like gene, YCA1, abrogates apoptosis and elevates oxidized proteins in Saccharomyces cerevisiae. *Proc. Natl. Acad. Sci. U.S.A.* **102,** 17326–17331
22. Cao, Y., Huang, S., Dai, B., Zhu, Z., Lu, H., Dong, L., Wang, Y., Gao, P., Chai, Y., and Jiang, Y. (2009) Candida albicans cells lacking CaMCA1-encoded metacaspase show resistance to oxidative stress-induced death and change in energy metabolism. *Fungal Genet. Biol.* **46,** 183–189
23. Shrestha, A., Puente, L. G., Brunette, S., and Megeney, L. A. (2013) The role of Yca1 in proteostasis. Yca1 regulates the composition of the insoluble proteome. *J. Proteomics* **81,** 24–30
24. Lee, R. E., Brunette, S., Puente, L. G., and Megeney, L. A. (2010) Metacaspase Yca1 is required for clearance of insoluble protein aggregates. *Proc. Natl. Acad. Sci. U.S.A.* **107,** 13348–13353
25. Lee, R. E., Puente, L. G., Kaern, M., and Megeney, L. A. (2008) A non-death role of the yeast metacaspase: Yca1p alters cell cycle dynamics. *PloS One* **3,** e2956
26. Silva, A., Almeida, B., Sampaio-Marques, B., Reis, M. I., Ohlmeier, S.,

Rodrigues, F., Vale, A., and Ludovico, P. (2011) Glyceraldehyde-3-phosphate dehydrogenase (GAPDH) is a specific substrate of yeast metacaspase. *Biochim. Biophys. Acta* **1813,** 2044–2049

27. Wu, X. Z., Chang, W. Q., Cheng, A. X., Sun, L. M., and Lou, H. X. (2010) Plagiochin E, an antifungal active macrocyclic bis(bibenzyl), induced apoptosis in Candida albicans through a metacaspase-dependent apoptotic pathway. *Biochim. Biophys. Acta* **1800,** 439–447
28. Aerts, A. M., Carmona-Gutierrez, D., Lefevre, S., Govaert, G., Francois, I. E., Madeo, F., Santos, R., Cammue, B. P., and Thevissen, K. (2009) The antifungal plant defensin RsAFP2 from radish induces apoptosis in a metacaspase independent way in Candida albicans. *FEBS Lett.* **583,** 2513–2516
29. Wilson, R. B., Davis, D., and Mitchell, A. P. (1999) Rapid hypothesis testing with Candida albicans through gene disruption with short homology regions. *J. Bacteriol.* **181,** 1868–1874
30. Lewicki, K., Marchand, S., Matoub, L., Lulek, J., Coulon, J., and Leroy, P. (2006) Development of a fluorescence-based microtiter plate method for the measurement of glutathione in yeast. *Talanta* **70,** 876–882
31. Inglis, D. O., Arnaud, M. B., Binkley, J., Shah, P., Skrzypek, M. S., Wymore, F., Binkley, G., Miyasato, S. R., Simison, M., and Sherlock, G. (2012) The Candida genome database incorporates multiple Candida species: multispecies search and analysis tools with curated gene and protein information for Candida albicans and Candida glabrata. *Nucleic Acids Res.* **40,** D667–674
32. Achcar, F., Camadro, J. M., and Mestivier, D. (2009) AutoClass@IJM: a powerful tool for Bayesian classification of heterogeneous data in biology. *Nucleic Acids Res.* **37,** W63–67
33. Crooks, G. E., Hon, G., Chandonia, J. M., and Brenner, S. E. (2004) WebLogo: a sequence logo generator. *Genome Res.* **14,** 1188–1190
34. Vacic, V., Iakoucheva, L. M., and Radivojac, P. (2006) Two Sample Logo: a graphical representation of the differences between two sets of sequence alignments. *Bioinformatics* **22,** 1536–1537
35. Colaert, N., Helsens, K., Martens, L., Vandekerckhove, J., and Gevaert, K. (2009) Improved visualization of protein consensus sequences by iceLogo. *Nat. Methods* **6,** 786–787
36. Phillips, A. J., Crowe, J. D., and Ramsdale, M. (2006) Ras pathway signaling accelerates programmed cell death in the pathogenic fungus Candida albicans. *Proc. Natl. Acad. Sci. U.S.A.* **103,** 726–731
37. Ojha, M., Cattaneo, A., Hugh, S., Pawlowski, J., and Cox, J. A. (2010) Structure, expression, and function of Allomyces arbuscula CDP II (metacaspase) gene. *Gene* **457,** 25–34
38. Watanabe, N., and Lam, E. (2005) Two Arabidopsis metacaspases AtMCP1b and AtMCP2b are arginine/lysine-specific cysteine proteases and activate apoptosis-like cell death in yeast. *J. Biol. Chem.* **280,** 14691–14699
39. Sundstrom, J. F., Vaculova, A., Smertenko, A. P., Savenkov, E. I., Golovko, A., Minina, E., Tiwari, B. S., Rodriguez-Nieto, S., Zamyatnin, A. A., Jr., Valineva, T., Saarikettu, J., Frilander, M. J., Suarez, M. F., Zavialov, A., Stahl, U., Hussey, P. J., Silvennoinen, O., Sundberg, E., Zhivotovsky, B., and Bozhkov, P. V. (2009) Tudor staphylococcal nuclease is an evolutionarily conserved component of the programmed cell death degradome. *Nat. Cell Biol.* **11,** 1347–1354
40. Tsiatsiani, L., Timmerman, E., De Bock, P. J., Vercammen, D., Stael, S., van de Cotte, B., Staes, A., Goethals, M., Beunens, T., Van Damme, P., Gevaert, K., and Van Breusegem, F. (2013) The Arabidopsis metacaspase9 degradome. *Plant Cell* **25,** 2831–2847
41. Zhu, J., Krom, B. P., Sanglard, D., Intapa, C., Dawson, C. C., Peters, B. M., Shirtliff, M. E., and Jabra-Rizk, M. A. (2011) Farnesol-induced apoptosis in Candida albicans is mediated by Cdr1-p extrusion and depletion of intracellular glutathione. *PloS One* **6,** e28830
42. Prasad, R., Shah, A. H., Sanwal, H., and Kapoor, K. (2012) Alanine scanning of all cysteines and construction of a functional cysteine-less Cdr1p, a multidrug ABC transporter of Candida albicans. *Biochem. Biophys. Res. Commun.* **417,** 508–513
43. Lee, J. Y., Yang, J. G., Zhitnitsky, D., Lewinson, O., and Rees, D. C. (2014) Structural basis for heavy metal detoxification by an Atm1-type ABC exporter. *Science* **343,** 1133–1136
44. Srinivasan, V., Pierik, A. J., and Lill, R. (2014) Crystal structures of nucleotide-free and glutathione-bound mitochondrial ABC transporter Atm1. *Science* **343,** 1137–1140
45. Fiori, A., Kucharikova, S., Govaert, G., Cammue, B. P., Thevissen, K., and Van Dijck, P. (2012) The heat-induced molecular disaggregase Hsp104 of Candida albicans plays a role in biofilm formation and pathogenicity in a worm infection model. *Eukaryotic Cell* **11,** 1012–1020
46. Madeo, F., Frohlich, E., Ligr, M., Grey, M., Sigrist, S. J., Wolf, D. H., and Frohlich, K. U. (1999) Oxygen stress: a regulator of apoptosis in yeast. *J. Cell Biol.* **145,** 757–767
47. Aerts, A. M., Zabrocki, P., Govaert, G., Mathys, J., Carmona-Gutierrez, D., Madeo, F., Winderickx, J., Cammue, B. P., and Thevissen, K. (2009) Mitochondrial dysfunction leads to reduced chronological lifespan and increased apoptosis in yeast. *FEBS Lett.* **583,** 113–117
48. Braun, R. J., Zischka, H., Madeo, F., Eisenberg, T., Wissing, S., Buttner, S., Engelhardt, S. M., Buringer, D., and Ueffing, M. (2006) Crucial mitochondrial impairment upon CDC48 mutation in apoptotic yeast. *J. Biol. Chem.* **281,** 25757–25767
49. Lefevre, S., Sliwa, D., Auchere, F., Brossas, C., Ruckenstuhl, C., Boggetto, N., Lesuisse, E., Madeo, F., Camadro, J. M., and Santos, R. (2012) The yeast metacaspase is implicated in oxidative stress response in frataxin-deficient cells. *FEBS Lett.* **586,** 143–148
50. Wissing, S., Ludovico, P., Herker, E., Buttner, S., Engelhardt, S. M., Decker, T., Link, A., Proksch, A., Rodrigues, F., Corte-Real, M., Frohlich, K. U., Manns, J., Cande, C., Sigrist, S. J., Kroemer, G., and Madeo, F. (2004) An AIF ortholog regulates apoptosis in yeast. *J. Cell Biol.* **166,** 969–974